Induction of tumor angiogenesis by Slit-Robo signaling and inhibition of cancer growth by blocking Robo activity

Biao Wang,[1,6] Yang Xiao,[1,6] Bei-Bei Ding,[1,6] Na Zhang,[1,3,6] Xiao-bin Yuan,[2] Lü Gui,[4] Kai-Xian Qian,[3] Shumin Duan,[2] Zhengjun Chen,[1] Yi Rao,[5] and Jian-Guo Geng[1,*]

[1]Laboratory of Molecular Cell Biology, Institute of Biochemistry and Cell Biology
[2]Institute of Neuroscience
Shanghai Institutes for Biological Sciences, Chinese Academy of Sciences, Shanghai 200031, China
[3]School of Life Sciences, Zhejiang University, Hangzhou, Zhejiang 310027, China
[4]Department of Pathology, Jinshan Hospital, Fudan University Medical Center, Shanghai, China
[5]Department of Anatomy and Neurobiology, Washington University School of Medicine, St. Louis, Missouri 63110
[6]These authors contributed equally to this work.
*Correspondence: jggeng@sunm.shcnc.ac.cn

Summary

Slit is a secreted protein known to function through the Roundabout (Robo) receptor as a chemorepellent in axon guidance and neuronal migration, and as an inhibitor in leukocyte chemotaxis. Here we show Slit2 expression in a large number of solid tumors and Robo1 expression in vascular endothelial cells. Recombinant Slit2 protein attracted endothelial cells and promoted tube formation in a Robo1- and phosphatidylinositol kinase-dependent manner. Neutralization of Robo1 reduced the microvessel density and the tumor mass of human malignant melanoma A375 cells in vivo. These findings demonstrate the angiogenic function of Slit-Robo signaling, reveal a mechanism in mediating the crosstalk between cancer cells and endothelial cells, and indicate the effectiveness of blocking this signaling pathway in treating cancers.

Introduction

Angiogenesis is a cellular process of capillary sprouting and configuring of neovasculature. It is of crucial importance in a variety of physiological and pathological conditions, including ischemia and hypoxia, wound healing, diabetic retinopathy, macular degeneration, neovascular glaucoma, psoriasis, rheumatoid arthritis, and cancer growth and metastasis (Hanahan and Folkman, 1996; Risau, 1997; Holash et al., 1999; Carmeliet and Jain, 2000). The obligatory requirement of angiogenesis for the growth and metastasis of cancers is now well recognized. For instance, the growth of solid tumors requires concomitant expansion of vascular networks to maintain the blood supply of oxygen and nutrients; an insufficient supply of blood (to tissues located more than 100 to 200 μm away from blood vessels) can lead to cancer necrosis. Although vascular endothelial cell growth factors (VEGFs), fibroblast growth factors (FGFs), and several other angiogenic molecules are indispensable for vessel formation (Gale and Yancopoulos, 1999; Yancopoulos et al., 2000; Folkman, 2001, 2002; Kerbel and Folkman, 2002), the molecular and cellular mechanisms regulating tumor angiogenesis are still not well understood.

Several families of extracellular proteins including the netrins, the semaphorins, the ephrins, and the Slits function as guidance cues to attract or repel projecting axons and migrating neurons during the development of the nervous system (Tessier-Lavigne and Goodman, 1996; Dickson, 2002). Slit is a new family of secreted repellents in axon guidance (Wang et al., 1999; Brose et al., 1999; Kidd et al., 1999; Li et al., 1999) and neuronal migration (Wu et al., 1999). The receptor for Slit is the transmembrane protein Roundabout (Robo) (Kidd et al., 1998, 1999; Brose et al., 1999; Li et al., 1999). Slit has recently been shown to be an endogenously available inhibitor of leukocyte chemotaxis (Wu et al., 2001). There are three Slits and four Robos in mammals (for a recent review, see Wong et al., 2002). Some of the Slits and Robos are expressed in adult tissues and outside the nervous system (Holmes et al., 1998; Wu et al., 2001). For example, *SLIT2* mRNA in endothelial cells and *ROBO1* mRNA in leukocytes have been reported (Wu et al., 2001). However, it has not been determined whether human cancer cells can express these genes, either at the mRNA or protein levels. Potential roles of Slit-Robo signaling in pathological conditions have been suggested (Wu et al., 2001), but not established. We

SIGNIFICANCE

Communication between tumor cells and vascular endothelial cells is known to be important in tumor-induced angiogenesis. Mechanistic understanding of tumor-induced angiogenesis is crucial for designing therapeutic approaches. Our results have revealed a previously unsuspected role of Slit-Robo signaling in tumor angiogenesis and shown the importance of this pathway in tumor growth. Interestingly, Slit attracts vascular endothelial cells, which is opposite to its roles as repellents and inhibitors in axon guidance and neuronal and leukocyte migration. These basic findings allowed us to design a strategy of neutralizing Robo1 activity for inhibition of tumor growth. Our results have uncovered a molecular mechanism for tumor-induced angiogenesis and led to the finding of a novel molecular target for controlling tumor growth.

have now investigated whether Slit and Robo could play roles in tumor angiogenesis in vitro and in vivo. Results from our current studies have established that Slit-Robo signaling attracts vascular endothelial cells, which significantly extends the previous conclusion of a fundamentally conserved mechanism for guiding somatic cell migration (Wu et al., 2001; Rao et al., 2002). Furthermore, our findings of Slit-Robo signaling in promoting tumor-induced angiogenesis indicate that Slit and Robo play significant roles in pathological conditions. The effectiveness of Robo blockade in limiting tumor growth demonstrates a novel target as well as molecular tools for cancer therapy.

Results

Expression of Slit2 on cancer cells and Robo1 in endothelial cells

Using reverse-transcription coupled to the polymerase chain reaction (RT-PCR), we found that A375 cells, a cell line derived from a human malignant melanoma, expressed *SLIT2* mRNA and human umbilical vein endothelial cells (HUVECs) expressed *ROBO1* mRNA, respectively (Figures 1A and 1D). The expression of *SLIT2* mRNA in A375 cells and *ROBO1* mRNA in HUVECs was confirmed by Northern blotting with ^{32}P-labeled *SLIT2* and *ROBO1* cDNA fragments (Figures 1B and 1E). The *G3PDH* mRNA, a house-keeping gene, was probed as the loading control of total input RNA. We generated antibodies to Slit2 and Robo1 and detected the expression of Slit2 protein in A375 cells (Figure 1C) and Robo1 protein in HUVECs (Figure 1F). Slit2/293 cells and Robo1/293 cells were used as the positive controls, and V/293 cells were used as the negative controls (Li et al., 1999; Wu et al., 1999; Wu et al., 2001). The expression of Slit2 in A375 cell derived solid tumors was detected by immunohistochemical staining with the anti-Slit2 antibody, but not with the preimmune IgG (Figure 1G). The expression of Robo1, which co-localized with vWF (von Willbrand factor) expression, in tumor endothelial cells was visualized with the anti-Robo1 antibody (Figure 1H), but not with the preimmune IgG (data not shown). Interestingly, there appeared to be a gradient of Slit2 protein with a higher concentration near the center of the tumor and a lower concentration in the periphery (Figure 1G). The expression of Slit2 in malignant melanoma and Robo1 in tumor endothelial cells suggests a possible paracrine Slit2/Robo1 interaction in the pathogenesis of malignant melanoma.

Cell surface localization of Slit2 and its upregulation

Although Slit2 is predicted to be a soluble protein, it has been shown to bind to Glypican-1 and to be localized on the cell surface in the brain, in a heparan sulfate proteoglycan (HSPG)-dependent manner (Liang et al., 1999; Hu, 2001; Ronca et al., 2001). Similarly, we found that the majority of Slit2 was associated with A375 cells in cell culture conditions, even though a small amount of Slit2 was also detected in the supernatants (Figure 1I). Pretreatment of A375 cells with heparin increased the amount of Slit2 in the supernatants and, at the same time, decreased the amount of Slit2 in the whole cell lysates, supporting the HSPG dependence for cell surface localization of Slit2 on A375 cells.

To explore the molecular mechanism governing the formation of the Slit2 gradient, we examined whether cytokines could regulate Slit2 expression in A375 cells. TNF-α (tumor necrosis factor-α) increased the expression of Slit2 (Figure 1I). Similar

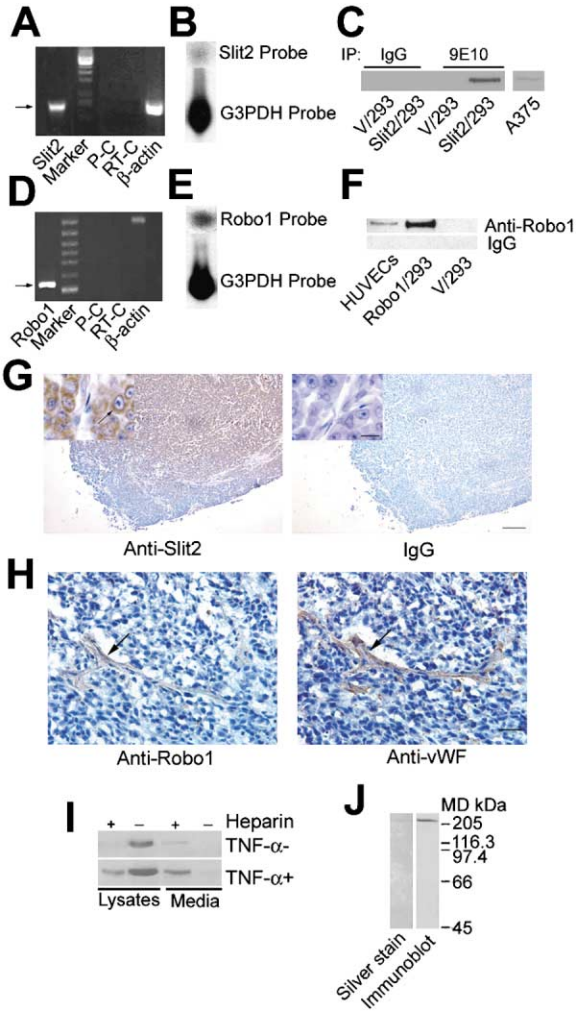

Figure 1. Expression of Slit2 in A375 cells and Robo1 in endothelial cells

A and **D:** *SLIT2* mRNA in A375 cells and *ROBO1* mRNA in HUVECs were determined by RT-PCR. Arrows indicated the positive *SLIT2* band (~1.0 kb) and *ROBO1* band (~500 bp), respectively. Human β-*ACTIN* mRNA (~1.0 kb) was also assayed as a control for RT-PCR. P-C (PCR control) lane was PCR in the absence of the templates; RT-C (RT control) was PCR using the template generated without the reverse transcriptase.

B and **E:** Northern blotting of *SLIT2* (~5.0 kb) in A375 cells and *ROBO1* (~4.6 kb) in HUVECs. *G3PDH* (a house-keeping gene; ~1.4 kb) was used as a loading control.

C and **F:** Protein expression of Slit2 in A375 cells (~200 kDa) and Robo1 (~200 kDa) in HUVECs was detected by anti-Slit2, anti-Robo1, and 9E10 Abs, but not by preimmune IgG. Slit2/293 cells and Robo1/293 cells were used as the positive control while V/293 cells were used as the negative control. 9E10 was a monoclonal antibody against the c-*myc* tag of Slit2 fusion protein.

G and **H:** Immunohistochemical staining of tumors with the anti-Slit2 Ab (an arrow indicated the expression of Slit2 on A375 cells; serial paraffin-embedding sections), with the anti-Robo1 Ab (an arrow indicated the expression of Robo1 on endothelial cells within the tumors; serial cryostat sections) or with preimmune IgG. The expression of Robo1 was colocalized with the vWF staining using an anti-vWF Ab. Scale bar, 100 μm for **G,** 20 μm for the inserts in **G,** and 50 μm for **H**.

I: Slit2 in the supernatants and the lysates of A375 cells without or with heparin and/or TNF-α.

J: Affinity-purified Slit2 was silver stained or immunoblotted with 9E10.

findings were also observed using IL-1β (interleukine-1β; data not shown), indicating that the upregulation of Slit2 in response to the secretion of proinflammatory mediators (and perhaps due to hypoxia or expression of oncogenes) could be involved in increasing Slit2 in the center of A375 cell-derived solid tumors, thus resulting in the generation of a gradient.

Attraction of endothelial cells by Slit2

We used several approaches to investigate whether and how Slit could regulate the migration of endothelial cells. We first tested whether Slit2 had any chemotactic effects on the migration of HUVECs using Boyden chamber assay. Similar to bFGF (basic fibroblast growth factor), purified recombinant human Slit2 protein (Figure 1J) induced the migration of HUVECs in a dose-dependent manner (Figure 2A). Preincubation of Slit2 with RoboN (an extracellular fragment of Robo1 that is a known inhibitor for the Slit2/Robo1 interaction; Wu et al., 1999, 2001) or preincubation of HUVECs with R5 (an IgG_{2b} monoclonal antibody to the first immunoglobulin domain of Robo1), but not with an IgG_{2b} control, significantly neutralized the Slit2-induced migration (Figures 2A and 2B). In contrast, RoboN or R5 did not affect the bFGF-induced migration of HUVECs. These results indicate that Slit2 can promote the migration of HUVECs through Robo1.

To determine the functional significance of Robo1, we performed reconstitution experiments using Robo1/293 cells. Slit2 and bFGF both promoted the migration of Robo1/293 cells, but RoboN only neutralized Slit2-induced, but not bFGF-induced, migration of Robo1/293 cells (Figure 2C). Furthermore, bFGF, but not Slit2, triggered the migration of V/293 cells, indicating that HEK293 cells express endogenous receptors for bFGF. Evidently, Robo1 is essential for the cell migration mediated by Slit2, but not mediated by bFGF, suggesting a specific role for Robo1 in mediating cellular responses to Slit2.

To determine whether Slit2 guided the direction of endothelial cell migration, rather than simply increasing the motility (nondirectional or random migration) of endothelial cells, we adopted a technique that had been successfully used for direct observation of axon projection (Song et al., 1997; Ming et al., 2002). This device could generate a microscopic gradient of a specific protein delivered in a picoliter volume through a micropipette by repetitive pressue (Höpker et al., 1999). We loaded a micropipette with Slit2 or bFGF protein and placed its tip at a distance of 100 μm away from the center of individual HUVECs. The entire trajectory of the migrating HUVECs was recorded in a timelapse microscopy. As shown in the examples (Figure 2D), the endothelial cell did not migrate when PBS (phosphate buffered saline, pH 7.4) was applied. However, it migrated toward the micropipette loaded with Slit2 in a time-dependent manner, indicating that Slit2 was a chemoattractant for HUVECs. In contrast, HUVECs could migrate toward or away from the micropipette loaded with bFGF in a time-dependent manner (an example of a cell migrating away from bFGF was shown in Figure 2D). The entire sets of experimental data could be presented as the cumulative distribution (%) versus migrated distance (μm; Figure 2E) and, alternatively, as the migrated distance (μm) versus the various treatment (Figure 2F). Cell migration toward a Slit2 gradient established an attractive role for the Slit2-induced endothelial cell migration (Figures 2D–2F). In contrast, bFGF increased the motility of HUVECs by inducing the migration of HUVECs; however, this migration was not directional (Figures 2D–2F). RoboN added in the bath neutralized the Slit2-induced directional migration, but had no inhibitory effect on the bFGF-induced migration (Figures 2E and 2F). These data indicate that Slit2 can attract the directional migration of vascular endothelial cells through Robo1.

Angiogenic activity of Slit2 and role of Slit2-Robo1 signaling in tumor-induced angiogenesis

To investigate the potential regulation of angiogenesis by Slit2, we first examined whether Slit2 could induce the differentiation, specifically tube formation of HUVECs in vitro. Slit2 increased the generation of tubular networks in a dose-dependent manner (Figures 2G and 2H). Preincubation of Slit2 with RoboN (Figures 2G and 2H), or preincubation of HUVECs with R5 (Figure 2I), neutralized the effect of Slit2, resulting in fewer and shorter tube structures. These results indicate that Slit2 has an angiogenic activity in vitro. It should be mentioned that Slit2 had no detectable activity on the proliferation of HUVECs (data not shown).

Because A375 cells expressed Slit2 and Slit2 induced the migration and the tube formation of endothelial cells in vitro, we tested the pathological significance of Slit2-Robo1 signaling in tumor angiogenesis using the xenografted animal model. For this purpose, we transfected A375 cells with the RoboN plasmid or the plain vector followed by antibiotic selection and single cell cloning. Using this approach, three stable single cell clones expressing RoboN (designated as RoboN/A375_C1, C2, and C3 cells) and one stable cell clone expressing the vector (designated as V/A375 cells) were generated. These clones were characterized by immunoblotting for RoboN, Slit2, and VEGF (β-tubulin as loading control) expression to ensure that the similar amounts of RoboN were expressed in all three C1, C2, and C3 clones and that no alterations of Slit2 and VEGF expression were detected among RoboN/A375_C1, C2, C3, and V/A375 clones (Figure 3A). In addition, they were tested for in vitro growth rates to ensure that they all grew at similar rates in cell culture conditions (Figure 3B).

These transfectants were then inoculated subcutaneously into athymic nude mice. When compared to those from V/A375 cells, tumors resulting from RoboN/A375_C1, C2, and C3 cells had significantly reduced microvessel densities (Figures 3C and 3D). Furthermore, the tumor volumes and masses from Robo1/A375_C1, C2, and C3 cells were all markedly smaller than those from the control V/A375 (Figures 3E and 3F).

As an alternative approach to the RoboN construct, we tested R5, the function-blocking monoclonal antibody against the first immunoglobulin motif of Robo1. RoboN would block Slit signaling by absorbing Slit proteins, whereas R5 should block Robo specifically, thereby providing a complementary approach to inhibit Slit2-Robo1 signaling. We found that, compared to an IgG_{2b} control, R5 clearly reduced tumor microvessel densities and tumor masses (Figures 3H–3M).

To substantiate the above conclusion, we further examined the effects of Slit2 overexpression in tumor angiogenesis and growth. We proposed that Slit2 overexpression could induce the exaggerated tumor angiogenesis and the accelerated expansion of tumor mass. After transfection of A375 cells with the Slit2 plasmid or the plain vector as described above, we generated two stable single cell clones expressing Slit2 (designated as Slit2/A375_C1 and C2 cells) and one stable cell clone expressing the vector (designated as V/A375 cells). They were characterized by immunoblotting for Slit2 and VEGF (β-tubulin

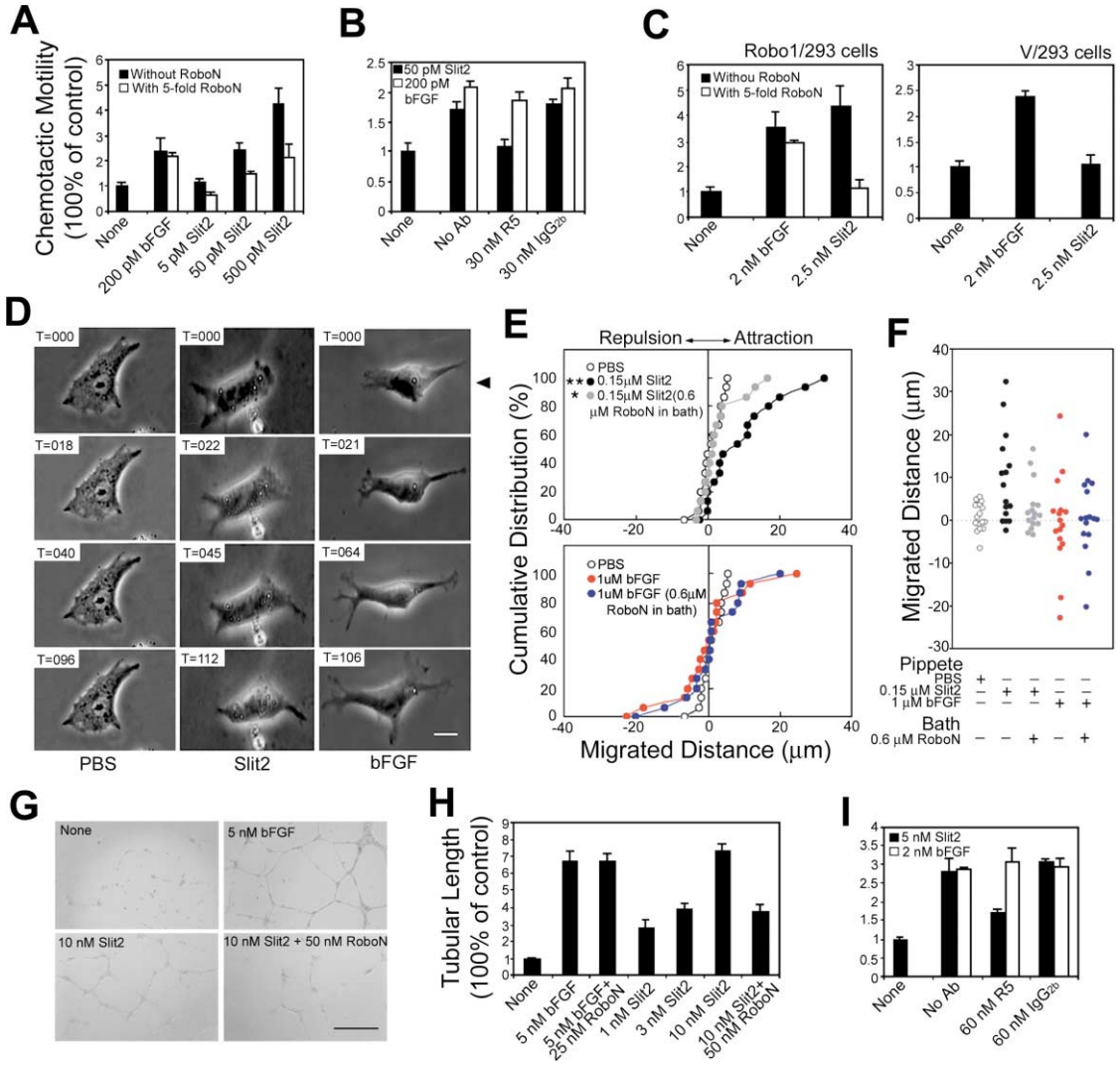

Figure 2. Slit2-induced migration and tube formation of endothelial cells

Migrations of HUVECs (**A** and **B**), Robo1/293 cells, and V/293 cells (**C**) were measured using Boyden chamber assay. Results were calculated as mean ± SD values from triplicate measurements of three to six separate experiments.

D: For measurement of directional migration of HUVECs, a protein gradient was applied from a micropipette by the pulsatile application of 0.15 μM Slit2 or 1 μM bFGF. Phase-contrast micrographs of endothelial cells were recorded in a timelapse mode after exposure to the Slit2 or bFGF gradients (min). The arrowhead indicated the direction in which the protein was loaded through the micropipette. Scale bar, 8 μm.

The migratory directions induced by Slit2 and bFGF (**E**) and migrated distances (**F**) were determined (each dot representing the migratory direction and distance of a single endothelial cell). *, $p < 0.05$ and **, $p < 0.01$, Kolmogorov-Smirnov test.

G: Tube formation of HUVECs on Matrigel was visualized by phase-contrast microscopy. Scale bar, 60 μm.

H and **I:** The effects of Slit2 and bFGF on the tube formation of HUVECs without or with RoboN or R5. Results were calculated as mean ± SD values from triplicate measurements of three separate experiments.

as loading control) expression to ensure that the similar amounts of Slit2 were overexpressed in both C1 and C2 clones and that no alterations of VEGF expression were detected among C1, C2, and V/A375 clones (Supplemental Figure S1A at http://www.cancercell.org/cgi/content/full/4/1/19/DC1). In addition, they were tested to ensure that they all grew at similar rates in cell culture conditions (Supplemental Figure S1B).

After inoculation of these transfectants, tumors resulting from Slit2/A375_C1 and C2 cells had significantly increased microvessel densities if compared to those from V/A375 cells (Supplemental Figures S1C and S1D on *Cancer Cell* website). Furthermore, the tumor volumes and masses from Slit2/A375_C1 and C2 cells were all significantly bigger than those from the control V/A375 (Supplemental Figures S1E and S1F). These in vivo results demonstrate the biological significance of Slit2-Robo1 signaling in tumor angiogenesis and growth.

As endothelial cells expressed both Slit2 and Robo1 and Slit2 reportedly inhibited leukocyte chemotaxis (Wu et al., 2001), we measured the leukocyte counts in the blood and in the solid tumors of these xenografted mice. We found no clear differences among these groups (Figures 3G and 3N and Supplemental Figure S1G). The equivalent numbers of leukocytes

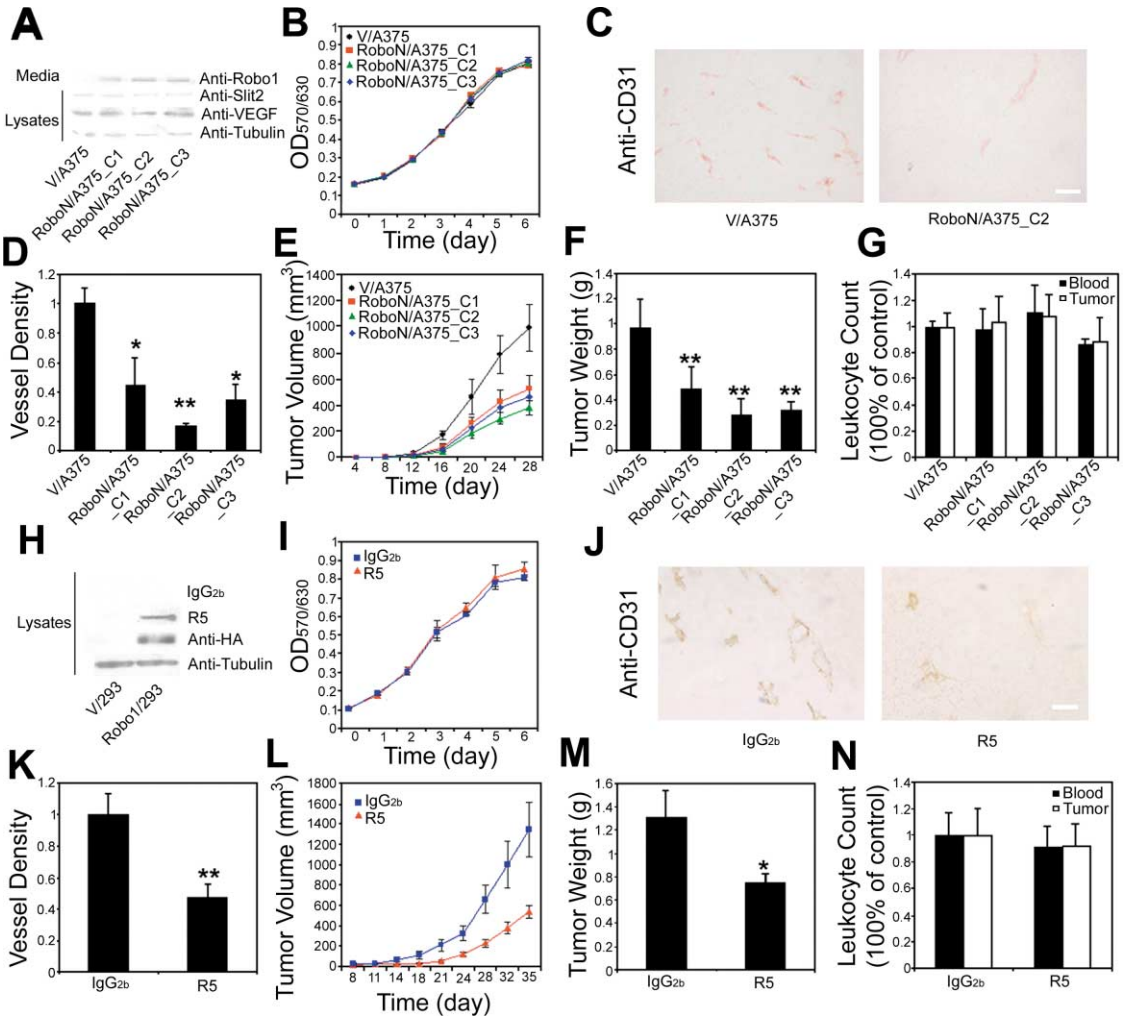

Figure 3. Inhibition of angiogenesis and growth of malignant melanoma

A: Detection of RoboN by the anti-Robo1 Ab in three single cell stable clones of RoboN/A375_C1, C2, and C3, but not in one single cell stable clone of V/A375. Slit2, VEGF, and β-tubulin were also detected by the respective Abs to Slit2, VEGF, and β-tubulin in all these cell clones. No signal was evident with preimmune rabbit IgG (data not shown).

H: R5, but not an IgG_{2b} control, recognized Robo1. The anti-HA (hemagglutinin) Ab (Clontech), which recognized the HA tag of Robo1 fusion protein in Robo1/293 cells, was used as the positive control.

B and **I:** Measurement of growth rates for V/A375 cells and RoboN/A375_C1, C2, and C3 cells (**B**) and for A375 cells in the presence of mouse IgG_{2b} or R5 (**I**). Results were expressed as the mean ± SD values from triplicate measurements of three separate experiments.

C and **J:** Immunohistochemical staining of blood vessels within tumors of V/A375 cells and RoboN/A375_C2 cells (**C**) and of A375 cells treated with mouse IgG_{2b} and R5 (**J**) using an anti-CD31 Ab. No positive staining was detected when preimmune IgG was used (data not shown). Scale bar, 20 μm.

D and **K:** The mean ± SD values of microvessel densities (CD31 staining) were statistically analyzed using the ImageTool software for tumors of V/A375 cells, RoboN/A375_C1, C2, and C3 cells (**D**) and of A375 cells treated with an IgG_{2b} control or R5 (**K**; n = 14 for each group).

E and **L:** The mean ± SD values of tumor volumes for tumors from V/A375 cells, RoboN/A375_C1, C2, and C3 cells (**E**) and from A375 cells treated with mouse IgG_{2b} or R5 (**L**; n = 14 for each group).

F and **M:** The mean ± SD values of tumor weights for tumors from V/A375 cells, RoboN/A375_C1, C2, and C3 cells (**F**) and from A375 cells treated with mouse IgG_{2b} or R5 (**M**; n = 14 for each group).

G and **N:** Leukocyte counts in blood and in tumors derived from V/A375 cells, RoboN/A375_C1, C2, and C3 cells (**G**) and from A375 cells treated with mouse IgG_{2b} or R5 (**N**; n = 14 for each group). *, $p < 0.05$ and **, $p < 0.01$, Student's t test.

within the tumors were further confirmed by hematoxylin and eosin (H&E) staining of the tissue sections (data not shown). Slit2 therefore does not appear to be involved in leukocyte trafficking into malignant melanoma in vivo.

Expression of Slit2 in human cancers

To explore the general significance of our findings, we examined the expression of Slit2 in multiple human cancer cell lines originating from various tissues and organs. Slit2 was expressed in A375 cells (malignant melanoma), SCaBER cells (bladder squamous carcinoma), SK-N-SH cells (neuroblastoma), NCI-H446 cells (small cell lung cancer), T24 cells (transitional cell carcinoma of urinary bladder), LoVo cells (colon adenocarcinoma), ZR-75-30 cells (breast cancer), CNE cells (nasopharyngeal carcinoma), SMMC-7721 cells (hepatocellular carcinoma), Acc-2 and Acc-M cells (both were adenoid cystic carcinoma of

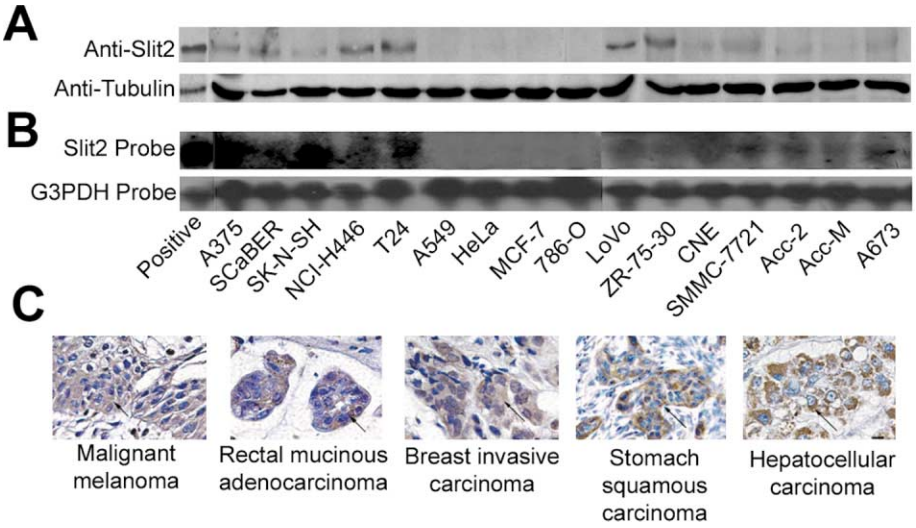

Figure 4. Expression of Slit2 in cancers

A: Immunoblotting of cell lysates from various cancer cell lines using the anti-Slit2 Ab and the anti-β-tubulin Ab. The Slit2/293 cells were used as the positive control.

B: Northern blotting of *SLIT2* and *G3PDH* mRNAs using ^{32}P-labeled *SLIT2* and *G3PDH* cDNA fragments. **C:** Immunohistochemical staining of various human cancers with the anti-Slit2 Ab. Arrows indicated the expression of Slit2 on tumor cells. Scale bar, 10 μm.

salivary gland), and A673 cells (rhabdomyosarcoma; Figure 4A). However, Slit2 was not detected in A549 cells (lung cancer), HeLa cells (cervical epithelial adenocarcinoma), MCF-7 cells (breast adenocarcinoma), and 786-O cells (primary renal cell adenocarcinoma). The expression of Slit2 in these cancer cell lines was confirmed by Northern blotting with ^{32}P-labeled *SLIT2* cDNA fragment (Figure 4B). Again, the β-tubulin immunoblotting and the *G3PDH* Northern blotting were used as the loading controls of input proteins and RNAs (Figures 4A and 4B).

The finding of Slit2 expression in a variety of cancer cell lines is consistent with the recent report of Slit2 expression in prostate cancers using a RT-PCR-based approach (Latil et al., 2003). Along this line of investigation, we examined human samples of malignant melanoma, rectal mucinous adenocarcinoma, invasive breast carcinoma, gastric squamous carcinoma, and hepatocellular carcinoma for Slit2 expression (Figure 4C). We found that in all these cancer samples, Slit2 was expressed in the cancerous tissues, but not in the nearby regions of apparently normal tissues. The positive staining of Slit2 was found in 3 malignant melanomas (n = 7), 51 breast carcinomas (n = 72; 70.8% positive), 42 colorectal carcinomas (n = 65; 64.6% positive), and 38 gastric carcinomas (n = 74; 51.4% positive). Notably, Slit2 staining appeared to be more intense in the areas of the tumor, where more cancer cells and blood vessels (visualized by an antibody to vWF) existed within human colon carcinoma (Figure 5A). In contrast, less Slit2 staining was detected where there were fewer cancer cells and vasculatures. A similar correlation was also found in human breast carcinoma (data not shown). Furthermore, Slit2 was absent in normal and hyperplastic colon tissues, began to appear in colon adenomas (3/14; 21.4% positive), and upregulated in colon carcinoma (42/65; 64.6% positive; Figure 5B). These data suggest a correlation among cancerous alterations, Slit2 expression, and the microvessel density within tumors.

Involvement of phosphatidylinositol-3 kinase (PI-3K) in Slit2-induced migration and tubulogenesis of endothelial cells

In an effort to explore downstream molecular mechanisms of the Slit2-Robo1 signaling in vascular endothelial cells, we screened a variety of chemicals for their effects on the migration and the tube formation of HUVECs induced by Slit2. We found that Wortmannin and LY294002 (both PI-3K inhibitors; Toker and Cantley, 1997; Fruman et al., 1998), but not KT5823 (an inhibitor of protein kinase G), attenuated Slit2-induced migration, but not bFGF-induced migration, of HUVECs in a dose-dependent manner (Figures 6A and 6B). Both inhibitors also attenuated directional migration (Figure 6E) and tubulogenesis induced by Slit2 (Figures 6C and 6D). Biochemically, Slit2, but not bFGF, could activate PI-3K in HUVECs, resulting in the increased radioactivity of ^{32}P-ATP-labeled inositol phospholipids (Figures 6F and 6G). These data demonstrate that activation of PI-3K in HUVECs by Slit2 is required for directional migration and tube formation of vascular endothelial cells.

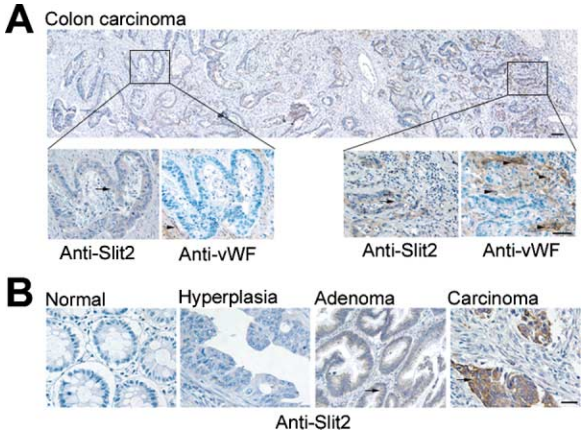

Figure 5. The correlation of Slit2 expression with MVD alterations and Slit2 expression in carcinoma stage

A: Immunohistochemical staining of human colon carcinoma with the anti-Slit2 and anti-vWF Abs. Arrows indicated the Slit2 expression on cancer cells and arrowheads indicated the microvessels within the solid tumors. Scale bar, 100 μm for the upper panel and 50 μm for the lower panel.

B: Immunohistochemical examination of the tissue sections from human colon adenoma (weak staining) and carcinoma (strong staining) using the anti-Slit2 Ab. No Slit2 staining for the normal or hyperplastic colon tissues. Scale bar, 50 μm.

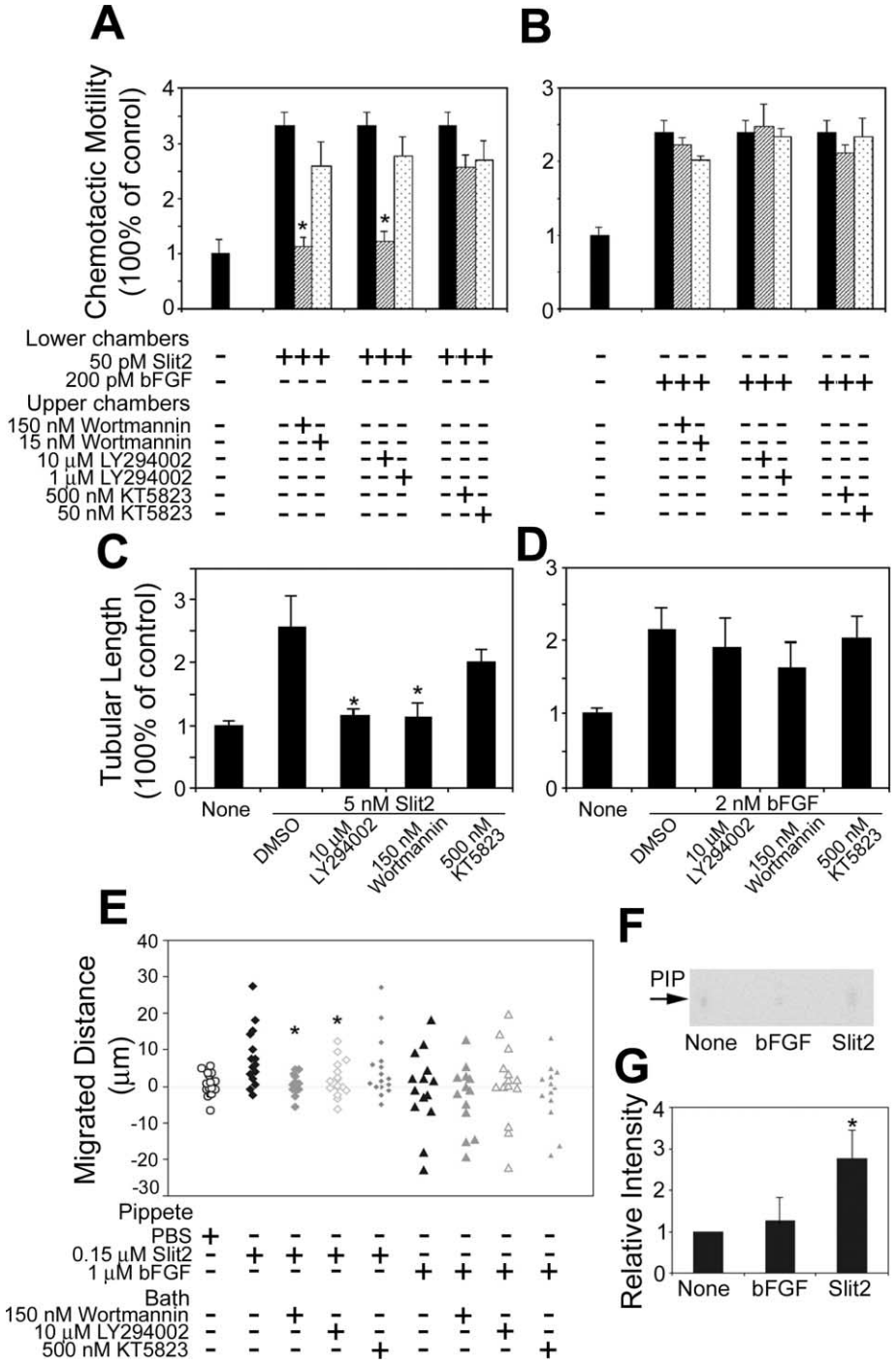

Figure 6. Requirement of PI-3K for Slit2-induced migration and tube formation of HUVECs

A and **B:** The migrations of HUVECs, without or with Wortmannin, LY294002, or KT5823, were measured when Slit2 (**A**) or bFGF (**B**) was present in the lower chambers using Boyden chamber assay. Results were calculated as mean ± SD values from triplicate measurements of three separate experiments.

C and **D:** The tube formations of HUVEC, in the absence or presence of inhibitors, were examined when Slit2 (**C**) or bFGF (**D**) was present. Results were calculated as mean ± SD values from triplicate measurements of three separate experiments.

E: The migrated distances of HUVECs without or with inhibitors were analyzed (each dot representing the migratory direction and distance of a single endothelial cell). *, $p < 0.05$, Kolmogorov-Smirnov test.

F: Following treatment of HUVECs with Slit2 or bFGF, PI-3K was precipitated and used to catalyze PI to ^{32}P-ATP-labeled phosphatidylinositol phosphalipids (PIP). The reactants were separated and visualized.

G: The means ± SD values of the radioactivity for the P^{32}-labeled PIP from three independent experiments. *, $p < 0.05$, Student's t test.

Discussion

Our results have concluded that in addition to its well-characterized functions in axon guidance and neuronal migration, Slit2 can attract vascular endothelial cells and promote tumor-induced angiogenesis. This strengthens the idea of fundamental conservation of guidance mechanisms for all somatic cells (Wu et al., 2001; Rao et al., 2002). Our results also indicate that Slit2 expressed in solid tumors can communicate with Robo1 expressed in endothelial cells, revealing a pathway mediating tumor-induced angiogenesis. Because we can inhibit tumor growth in vivo by specific neutralization of the Slit2-Robo1 interaction with either the extracellular part of Robo1 or R5, the function-blocking monoclonal antibody for Robo1, it not only indicates the importance of Slit-Robo signaling in tumor-induced angiogenesis and tumor growth, but also provides novel molecular tools for attenuating tumors. Taken together, our results have significant implications in both basic mechanisms and clinical applications.

Migratory behavior is distinct among different cell types,

with different speeds and different morphologies. Previously, distinct guidance cues have been found for different cells, with chemotactic factors functioning through seven transmembrane G protein-coupled receptors (GPCRs) discovered to be important for nonneuronal cells and guidance cues functioning through single transmembrane receptors shown to be important for neurons. Only recently have neuronal guidance cues been found to directly guide the migration of leukocytes (Wu et al., 2001) while leukocyte chemotactic factors were shown to function directly on neurons (Lu et al., 2001, 2002; Klein et al., 2001; Zhu et al., 2002; Xiang et al., 2002). Those findings based on neurons and leukocytes led to the proposal of the idea of conserved molecular mechanisms among all somatic cell types (Wu et al., 2001; Rao et al., 2002). Results reported in the present study significantly strengthen the idea by extending the conservation to vascular endothelial cells and to pathological processes.

All previous studies of Slits in neurons and leukocytes indicate that Slits are repulsive or inhibitory for migrating cells (recently reviewed in Wong et al., 2002). It is thus curious that Slit2 has been found to function as a chemoattractant for vascular endothelial cells. Previous studies by Poo and colleagues have shown that the same guidance cue can either attract or repel the same axons depending on intracellular cAMP and cGMP levels (Song et al., 1997). It will be interesting to test whether cAMP and cGMP play a role in endothelial cell migration and angiogenesis, in addition to their roles in endothelial responses to Slit2.

We have found that PI-3K is involved in endothelial cell responses to Slit2. It will be interesting to compare the pathways mediating attractive responses in endothelial cells to those in neurons, although the intracellular transduction pathway for Slit-Robo signaling in neuronal repulsion is only beginning to emerge (Bashaw et al., 2000; Fritz and VanBerkum, 2000; Wong et al., 2001). For example, it would be interesting to know whether PI-3K inhibitors, such as Wortmannin and LY294002, could prevent the repellant action of Slit2 on axon guidance and neuronal migration, and the inhibitory action of Slit2 on leukocyte chemotaxis.

Extensive studies of genetically engineered mouse models of spontaneous tumorigenesis and pathological examinations of human cancers have delineated discrete stages of carcinogenesis, including pre-angiogenic hyperplasia/dysplasia/carcinoma in situ (CIS), angiogenic dysplasia/CIS, and small tumor and large tumor/invasive carcinoma (Hanahan and Folkman, 1996). Among these stages, angiogenesis is switched on during the premalignant stage of tumor development, persisting thereafter. Although VEGF-mediated signaling is generally believed to be essential for the angiogenic switch, the expression of VEGF and its cognate receptors, flt-1 (VEGF-R1) and flk-1 (VEGF-R2), appears to be constitutive; no alterations in the expression of these molecules can be clearly detected (Bergers et al., 1999, 2000; Inoue et al., 2002). The disappointing results from the clinical trial using several inhibitors for VEGF and its receptors are consistent with the notion that other angiogenic factors are playing critical and indispensable roles in tumor angiogenesis (Kerbel and Folkman, 2002). Our finding of the Slit2 expression on cancerous tissues (Figure 5B) suggests that Slit2 is a novel player in tumorigenesis.

It should be pointed out that we have screened and found the increased Slit2 expression in a number of tumor cell lines and primary tumors in this study. However, there are two other Slits (Wong et al., 2002), which have not been tested in tumors. It is possible that Slit1 and Slit3 could also be expressed in some tumors. Similarly, we have so far focused on Robo1, whereas there are three other Robos. Considering the possibility that different Robos could be involved in angiogenesis, we suspect that RoboN (made from the extracellular part of Robo1) may block all three Slits and that the R5 antibody (made by immunization of and screening against the first immunoglobulin domain of Robo1) may block other Robos as well as Robo1.

The result of immunohistochemical staining suggests that Slit2 protein is expressed in a center-to-periphery gradient in solid tumors. It will be interesting to investigate whether this gradient contributes to the exaggerated angiogenesis in the center of solid tumors and what is the mechanism for forming and maintaining the Slit2 gradient. It has been reported that Slit2 associates with HSPGs on Glypican-1 expressed on the neuronal cells in the central nervous system. Likewise, the gradient formation of Hedgehog requires Tout-velu, an enzyme involved in HSPG biosynthesis (Bellaiche and Perrimon, 1998). Further, overexpression of the glypican HSPG, called Dally-like, leads to higher than normal levels of extracellular Wingless (Wg) accumulation (Tsuda et al., 1999). In contrast, clones defective in HSPG biosyhthesis bind to lower than normal levels of extracellular Wg and are deficient in Wg signaling (Baeg et al., 2001). Notum, a member of the α/β-hydrolase superfamily, influences the distribution of Wg by modifying HSPG Dally-like and Dally (Girádex et al., 2002). Our finding that pretreatment of A375 cells with heparin increases the amount of Slit2 in the supernatants and, at the same time, decreases the amount of Slit2 in the whole cell lysates also supports the association of Slit2 with HSPGs on cancer cells. It remains to be determined whether Slit2 is associated with Glypican-1 HSPGs expressed on cancer cells, whether regulation of Glypican-1 HSPGs alters the temporal and spatial distribution of Slit2 on cancer solids, and whether Tout-velu and/or Notum could affect the surface localization of Slit2 by modulating Glypican-1 HSPGs.

The results presented here have demonstrated the role of Slit2-Robo1 signaling in tumor angiogenesis and have evaluated the significance of this signaling pathway in the pathogenesis of cancers. However, whether this discovery can be translated to the diagnosis, treatment, and prevention of malignant tumors remains to be determined. For example, can the immunohistochemical staining of Slit2 be used as a reliable marker for the diagnosis of certain cancers? Are the measurements of Slit2 in the blood and the urine useful for screening certain carcinomas? Considering that the neutralization of Robo1 activity incompletely reduces the microvessel density and the tumor mass of malignant melanoma (Figure 3), it will be interesting to test the efficacy of a combined therapy using inhibitors for both VEGF and Slit2 for treatment of cancers. It is also interesting to test whether Slit2 has any synergistic effects on the angiogenic activities of VEGF, FGF, ephrin, and other known angiogenic factors.

Experimental procedures

RT-PCR and Northern blotting

Primary HUVECs were cultured as previously described (Geng et al., 1990). RT-PCR was performed as before (Ma and Geng, 2000). Primers used were human *SLIT2* sense (+3611) 5′-GGT GAC GGA TCC CAT ATC GCG GTA GAA CTC-3′ and antisense (−4574) 5′-GGA CAC CTC GAG CGT ACA GCC GCA CTT CAC-3′; human *ROBO1* sense (+4440) 5′-CCT ACA CAG ATG ATC TTC C-3′ and antisense (−4956) 5′-CAG AGG AGC CTG CAG CTC

AGC TTT CAG TTT CCT C-3′; human β-*ACTIN* sense (+1) 5′-ATG GAT GAT GAT ATC GCC GC-3′ and antisense (−1127) 5′-CTA GAA GCA TTT GCG GTG G-3′. Total RNAs from A375 cells and the primary culture of HUVECs were also probed with the ^{32}P-labeled human *Slit2* (1 kb), rat *ROBO1* (2.1 kb), or human *G3PDH* (1.3 kb) cDNA fragments.

Cell lines

Stable human embryonic kidney 293 cell lines expressing full-length human Slit2 with a c-*myc* tag at its carboxyl terminus (Slit2/293 cells), the extracellular portion of rat Robo1 (RoboN/293 cells) and full-length of rat Robo1 (Robo1/293 cells) with a HA tag at their carboxyl termini, and the plain vector (V/293 cells) were established as previously described (Li et al., 1999; Wu et al., 1999, 2001).

Antibody generation, immunoblotting, and immunostaining

GST and His-tag fusion proteins of Slit2 (encoding 57–207 or 1272–1593 amino acids of human *Slit2*) and Robo1 (encoding 1–168 or 961–1217 amino acids of rat *Robo1*) were constructed into pGEX-4T-1 (Amersham Pharmacia Biotech) and pET-30a(+) (Novagen) vectors and expressed according to the manufacturers' protocols. The purified GST fusion proteins were used as the antigens to immunize rabbits and mice for generation of anti-Slit2 and anti-Robo1 polyclonal and monoclonal antibodies. The purified His-tag fusion proteins were used for affinity isolation of the polyclonal antibodies and for ELISA assay during the screening of monoclonal antibodies. Equal amounts of cell lysates (routinely verified by β-tubulin immunoblotting; Sigma) were used for immunoblotting. For experiments of TNF-α or heparin treatment, A375 cells were cultured in the presence of either 300 units/ml TNF-α, 50 μg/ml heparin, or both for 12 hr. Antibodies against CD31 (PharMingen; a 1:50 dilution for cryostat sections), vWF (Antibody Diagnostica Inc.; a 1:200 dilution for paraffin-embedding and cryostat sections), Slit2 (5 μg/ml for paraffin-embedding sections), and Robo1 (20 μg/ml for cryostat sections) were used for immunohistochemical staining, as described before (Liu et al., 2001).

Isolation of Slit2 and RoboN

Recombinant Slit2 and RoboN proteins were purified from the conditioned medium by affinity chromatography using a 9E10 mAb to the c-*myc* tag (~1 mg/ml Affi-Gel 10; Bio-Rad) or a HA11 mAb to HA, HA11 (BAbCO). Purified Slit2 was silver stained and immunoblotted as before (Geng et al., 1997).

Boyden chamber assay

The cell migration assay (Gho et al., 1999) was conducted in a 48-well microchemotaxis chamber (Neuro Probe, Inc.). PVP-free polycarbonate membranes (8 μm pores) were coated with 1% gelatin. The bottom chambers were loaded with or without Slit2 or bFGF (Sigma), while the upper chambers were seeded with HUVECs (5×10^5 cells/ml), Robo1/293 cells (1×10^5 cells/ml), or V/293 cells (5×10^5 cells/ml) resuspended in M199 medium or DMEM supplemented with 1% heat inactivated fetal calf serum (FCS). For the RoboN inhibition experiments, Slit2 was mixed with 5-fold RoboN in a molar ratio at 4°C before adding to the bottom chambers. For antibody or chemical inhibition experiments, HUVECs were pretreated with the indicated amounts of mouse IgG_{2b}, R5, or chemical inhibitors at 37°C for 30 min, prior to adding to the upper chambers. They were incubated at 37°C for 4 hr. The filters were then fixed, stained with 0.5% crystal violet, and the cells that had migrated through the filters were counted.

Directional migration assay

The microscopic gradients of proteins were produced as described (Höpker et al., 1999). Briefly, a repetitive pressure injection of picoliter volumes of 0.15 μM Slit2 or 1 μM bFGF was applied through a micropipette with a tip at the opening of ~1 μm. The 24-well culture plate was coated with a thin layer of Matrigel (Becton Dickinson Labware) and the test cells were allowed to settle and to loosely attach to Matrigel. The experiments were carried out at 37°C in the presence of 5% CO_2. The pipette tip was placed 100 μm away from the center of any given cell under testing. Microscopic images were recorded, in a timelapse mode, with a CCD camera (JVC) attached to a phase contrast microscope (Olympus IX70) and stored in a computer for the detailed analysis using NIH Image. The migration distances of HUVECs at 2 hr were analyzed. The inhibition experiments of RoboN or chemical inhibitors were carried out as above.

Tube formation assay

96-well cell culture plates were coated with 100 μl/well of Matrigel and incubated at 37°C for 30 min to promote gelling (Malinda et al., 1999). HUVECs (passages 2 to 3) were resuspended at 1.3×10^5 cells per well in M199 medium supplemented with 2% heat-inactivated fetal calf serum. Aliquots of cells (0.1 ml per aliquot) were added to each Matrigel-containing well. The tubular structures were identified and photographed at 12 to 18 hr. The inhibition experiments of RoboN, R5, or chemical inhibitors were carried out as above.

Xenografted tumor growth model

A375 cells were transfected with the RoboN plasmid (RoboN/A375 cells), the Slit2 plasmid (Slit2/A375 cells), or the plain vector (V/375 cells) using Lipofectin™ (Gibco) and selected by 400 μg/ml hygromycin B (Sigma). The stable single cell clones of RoboN/A375_C1, C2, and C3 cells, Slit2/A375_C1 and C2 cells as well as V/A375 cells were verified by immunoblotting with antibodies against Robo1, Slit2, VEGF, and β-tubulin (as the loading control). They were resuspended at 5×10^6 cells/ml and an aliquot of 0.2 ml cell suspension was injected subcutaneously into athymic nude mice (O'Reilly et al., 1997). For antibody inhibition experiments, mice bearing A375 cell tumors were treated with intraperitoneal injections of R5 or an IgG_{2b} control twice per week (1 mg per injection). Tumor volumes were determined by external measurements and calculated according to the equation, $V = [L \times W^2] \times 0.52$ (V = volume, L = length, and W = width). Mice were sacrificed 28–35 days later. Mouse blood was collected before sacrifice for leukocyte counts, and myeloperoxidase activity for quantification of neutrophils within the tumors was performed (Wang et al., 2002).

Cell proliferation assay

All transfectants were grown in exponential phase and detached by trypsin treatment. Viable cells (5×10^4 cells/ml) were plated into 96-well tissue culture plates (100 μl complete medium/well) and cultured at 37°C in 5% CO_2 atmosphere. At different time points, tetrazolium salt was added (20 μl/well) and incubated at 37°C for 4 hr. The insoluble blue formazan product was solubilized by addition of 100 μl/well 10% SDS/5% isobutanol. The plates were read on a microtiter plate reader using a test wavelength of 570 nm and a reference wavelength of 630 nm.

Measurements of PI-3K activity

PI-3K activity assay was carried out as described before (Wallasch et al., 1995). HUVECs were starved in a M199 medium containing 2% FCS for 2 hr and then stimulated with 10 ng/ml Slit2 at 22°C for 15 min.

Acknowledgments

We thank Li-Ping Liu, Hai-Bo Wang, Hai-Xiong Han, Xiao-Feng Niu, Qin Cai, and Ji-Guo Liu for technical assistance. We are grateful to Dr. Gang Pei for teaching us Boyden chamber assay and for many constructive comments during this study. This study was supported by grants from Chinese Academy of Sciences (KSCX2-2-02), National Science Foundation of China (39925015, 30130090, and 30270649), Special Funds for Major State Basic Research of China (G1999053907), and 973 Program (2002CB513000) from Chinese Ministry of Science and Technology.

Received: March 24, 2003
Revised: June 2, 2003
Published: July 21, 2003

References

Baeg, G.H., Lin, X., Khare, N., Baumgartner, S., and Perrimon, N. (2001). Heparan sulfate proteoglycans are critical for the organization of the extracellular distribution of Wingless. Development *128*, 809–815.

Bashaw, G.J., Kidd, T., Murray, D., Pawson, T., and Goodman, C.S. (2000). Repulsive axon guidance: Abelson and Enabled play opposing roles downstream of the Roundabout receptor. Cell *101*, 703–715.

Bellaiche, Y., and Perrimon, N. (1998). Tout-velu is a *Drosophila* homologue

of the putative tumour suppressor EXT-1 and is needed for Hh diffusion. Nature *394*, 85–88.

Bergers, G., Javaherian, K., Lo, K.M., Folkman, J., and Hanahan, D. (1999). Effects of angiogenesis inhibitors on multistage carcinogenesis in mice. Science *284*, 808–812.

Bergers, G., Brekken, R., McMahon, G., Vu, T.H., Itoh, T., Tamaki, K., Tanzawa, K., Thorpe, P., Itohara, S., Werb, Z., and Hanahan, D. (2000). Matrix metalloproteinase-9 triggers the angiogenic switch during carcinogenesis. Nat. Cell Biol. *2*, 435–439.

Brose, K., Bland, K.S., Wang, K.H., Arnott, D., Henzel, W., Goodman, C.S., Tessier-Lavigne, M., and Kidd, T. (1999). Slit proteins bind Robo receptors and have an evolutionarily conserved role in repulsive axon guidance. Cell *96*, 795–806.

Carmeliet, P., and Jain, R.K. (2000). Angiogenesis in cancer and other disease. Nature *407*, 249–257.

Dickson, B.J. (2002). Molecular mechanisms of axon guidance. Science *298*, 1959–1964.

Folkman, J. (2001). Angiogenesis-dependent diseases. Semin. Oncol. *28*, 536–542.

Folkman, J. (2002). Role of angiogenesis in tumor growth and metastasis. Semin. Oncol. *29*, 15–18.

Fritz, J.L., and VanBerkum, M.F.A. (2000). Calmodulin and Son of sevenless dependent signaling pathways regulate midline crossing of axon in the *Drosophila* CNS. Development *127*, 1991–2000.

Fruman, D.A., Meyers, R.E., and Cantley, L.C. (1998). Phosphoinositide kinases. Annu. Rev. Biochem. *67*, 481–507.

Gale, N.W., and Yancopoulos, G.D. (1999). Growth factors acting via endothelial cell-specific receptor tyrosine kinases: VEGFs, Angiopoietins, and Ephrins in vascular development. Genes Dev. *13*, 1055–1066.

Geng, J.-G., Bevilacqua, M.P., Moore, K.L., McIntyre, T.M., Prescott, S.M., Kim, J.M., Bliss, G.A., Zimmerman, G.A., and McEver, R.P. (1990). Rapid neutrophil adhesion to activated endothelium mediated by GMP-140. Nature *343*, 757–760.

Geng, J.-G., Raub, T.J., Baker, C.A., Sawada, G.A., Ma, L., and Elhammer, Å.P. (1997). Expression of a P-selectin ligand in zona pellucida of porcine oocytes and P-selectin on acrosomal membrane of porcine sperm cells. Potential implications for their involvement in sperm-egg interactions. J. Cell Biol. *137*, 743–754.

Gho, Y.S., Kleinman, H.K., and Sosne, G. (1999). Angiogenic activity of human soluble intercellular adhesion molecule-1. Cancer Res. *59*, 5128–5132.

Girádex, A.J., Copley, R.R., and Cohen, S.M. (2002). HSPG modification by the secreted enzyme Notum shapes the wingless morphogen gradient. Dev. Cell *2*, 667–676.

Hanahan, D., and Folkman, J. (1996). Patterns and emerging mechanisms of the angiogenesis switch during tumorigenesis. Cell *86*, 353–364.

Holash, L., Maisonpierre, P.C., Compton, D., Boland, P., Alexander, C.R., Zagzag, D., Yancopoulos, G.D., and Weigand, S.J. (1999). Vessel cooption, regression, and growth in tumors mediated by Angiopoietins and VEGF. Science *284*, 1994–1998.

Holmes, G.P., Negus, K., Burridge, L., Raman, S., Algar, E., Yamada, T., and Little, M.H. (1998). Distinct but overlapping expression patterns of two vertebrate *slit* homologs implies functional roles in CNS development and organogenesis. Mech. Dev. *79*, 57–72.

Höpker, V.H., Shewan, D., Tessier-Lavigne, M., Poo, M.-M., and Holt, C. (1999). Growth-cone attraction to netrin-1 is converted to repulsion by laminin-1. Nature *401*, 69–73.

Hu, H. (2001). Cell-surface heparan sulfate is involved in the repulsive guidance activities of Slit2 protein. Nat. Neurosci. *4*, 695–701.

Inoue, M., Hager, J., Ferrara, N., Gerber, H.P., and Hanahan, D. (2002). VEGF-A has a critical, nonredundant role in angiogenic switching and pancreatic cell carcinogenesis. Cancer Cell *1*, 193–202.

Kerbel, R., and Folkman, J. (2002). Clinical translation of angiogenesis inhibitors. Nat. Rev. Cancer *2*, 727–739.

Kidd, T., Brose, K., Mitchell, K.J., Fetter, R.D., Tessier-Lavigne, M., Goodman, C.S., and Tear, G. (1998). Roundabout controls axon crossing of the CNS midline and defines a novel subfamily of evolutionarily conserved guidance receptors. Cell *92*, 205–215.

Kidd, T., Bland, K.S., and Goodman, C.S. (1999). Slit is the midline repellent for the Robo receptor in *Drosophila*. Cell *96*, 785–794.

Klein, R.S., Rubin, J.B., Gibson, H.D., DeHaan, E.N., Alvarez-Hernandez, X., Segal, R.A., and Luster, A.D. (2001). SDF-1α induces chemotaxis and enhances Sonic hedgehog-induced proliferation of cerebellar granule cells. Development *128*, 1971–1981.

Latil, A., Chene, L., Cochant-Priollet, B., Mangin, P., Fournier, G., Berthon, P., and Cussenot, O. (2003). Quantification of expression of netrins, slits and their receptors in human prostate tumors. Int. J. Cancer *103*, 306–315.

Li, H.S., Chen, J.H., Wu, W., Fagaly, T., Zhou, L.J., Yuan, W.L., Dupuis, S., Jiang, Z.H., Nash, W., Gick, C., et al. (1999). Vertebrate Slit, a secreted ligand for the transmembrane protein Roundabout, is a repellent for olfactory bulb axons. Cell *96*, 807–818.

Liang, Y., Annan, R.S., Carr, S.A., Popp, S., Mevissen, M., Margolis, R.K., and Margolis, R.U. (1999). Mammalian homologues of the Drosophila slit protein are ligands of the heparan sulfate proteoglycan glypican-1 in brain. J. Biol. Chem. *274*, 17885–17892.

Liu, L.-P., Xia, Y.-F., Yang, L., DiDonato, J.A., DiCorleto, P.E., Zhong, C.-P., and Geng, J.-G. (2001). B lymphocytes and plasma cells express functional E-selectin by constitutive activation of NF-κB. Biochem. Biophys. Res. Commun. *286*, 183–191.

Lu, Q., Sun, E., Klein, R.S., and Flanagan, J.G. (2001). Ephrin-B reverse signaling is mediated by a novel PDZ-RGS protein and selectively inhibits G protein-coupled chemoattraction. Cell *105*, 69–79.

Lu, M., Grove, E.A., and Miller, R.J. (2002). Abnormal development of the hippocampal dentate gyrus in mice lacking the CXCR4 chemokine receptor. Proc. Natl. Acad. Sci. USA *99*, 7090–7095.

Ma, Y.-Q., and Geng, J.-G. (2000). Heparan sulfate-like proteoglycans mediate adhesion of human malignant melanoma A375 cells to P-selectin under flow. J. Immunol. *165*, 558–565.

Malinda, K.M., Nomizu, M., Chung, M., Delgado, M., Kuratomi, Y., Yamada, Y., Kleinman, H.K., and Ponce, M.L. (1999). Identification of laminin α1 and β1 chain peptides active for endothelial cell adhesion, tube formation, and aortic sprouting. FASEB J. *13*, 53–62.

Ming, G.-L., Wang, S.T., Henley, J., Yuan, X.-B., Song, H.-J., Spitzer, N.C., and Poo, M.-M. (2002). Adaption in the chemotactic guidance of nerve growth cones. Nature *417*, 411–418.

O'Reilly, M.S., Boehm, T., Shing, Y., Fukai, N., Vasios, G., Lane, W.S., Flynn, E., Birkhead, J.R., Olsen, B.R., and Folkman, J. (1997). Endostatin: an endogenous inhibitor of angiogenesis and tumor growth. Cell *88*, 277–285.

Rao, Y., Wong, K., Ward, M., Jurgensen, C., and Wu, J.Y. (2002). Neuronal migration and molecular conservation with leukocyte chemotaxis. Genes Dev. *16*, 2973–2984.

Risau, W. (1997). Mechanisms of angiogenesis. Nature *386*, 671–674.

Ronca, F., Andersen, J.S., Paech, V., and Margolis, R.U. (2001). Characterization of Slit protein interactions with glypican-1. J. Biol. Chem. *276*, 29141–29147.

Song, H.-J., Ming, G.-L., and Poo, M.-M. (1997). A cAMP-induced switching of turning direction of nerve growth cones. Nature *388*, 275–279.

Tessier-Lavigne, M., and Goodman, C.S. (1996). The molecular biology of axon guidance. Science *274*, 1123–1133.

Toker, A., and Cantley, L.C. (1997). Singalling through the lipid products of phosphoinostidide-3-OH kinase. Nature *387*, 673–676.

Tsuda, M., Kamimura, K., Nakato, H., Archer, M., Staatz, W., Fox, B., Humphrey, M., Olson, S., Futch, T., Kaluza, M., et al. (1999). The cell-surface

proteoglycan Dally regulates Wingless signaling in *Drosophila*. Nature *400*, 276–280.

Wallasch, C., Weiss, F.U., Niederfellner, G., Jallal, B., Issing, W., and Ullrich, A. (1995). Heregulin-dependent regulation of HER2/neu oncogenic signaling by heterodimerization with HER3. EMBO J. *14*, 4267–4275.

Wang, K.H., Brose, K., Arnott, D., Kidd, T., Goodman, C.S., Henzel, W., and Tessier-Lavigne, M. (1999). Biochemical purification of a mammalian Slit protein as a positive regulator of sensory axon elongation and branch. Cell *96*, 771–784.

Wang, J.-G., Mu, J.-S., Zhu, H.-S., and Geng, J.-G. (2002). N-desulfated non-anticoagulant heparin inhibits leukocyte adhesion and transmigration in vitro and attenuates acute peritonitis and ischemia and reperfusion injury in vivo. Inflamm. Res. *51*, 435–443.

Wong, K., Ren, X.R., Huang, Y.Z., Xie, Y., Liu, G., Saito, H., Tang, H., Wen, L., Brady-Kalnay, S.M., Mei, L., et al. (2001). Signal transduction in neuronal migration: roles of GTPase activating proteins and the small GTPase Cdc42 in the Slit-Robo pathway. Cell *107*, 209–221.

Wong, K., Park, H.T., Wu, J.Y., and Rao, Y. (2002). Slit proteins: guidance cues for cells ranging from neurons to leukocytes. Curr. Opin. Genet. Dev. *12*, 583–591.

Wu, W., Wong, K., Chen, J.H., Jiang, Z.H., Dupuis, S.M., Wu, J.Y., and Rao, Y. (1999). Directional guidance of neuronal migration in the olfactory system by the protein Slit. Nature *400*, 331–336.

Wu, J.Y., Feng, L.L., Park, H.T., Havlioglu, N., Wen, L., Tang, H., Bacon, K.B., Jiang, Z.H., Zhang, X.C., and Rao, Y. (2001). The Neuronal repellent Slit inhibits leukocyte chemotaxis induced by chemotactic factors. Nature *410*, 948–952.

Xiang, Y., Li, Y., Zhang, Z., Cui, K., Wang, S., Yuan, X.B., Wu, C.P., Poo, M.-M., and Duan, S. (2002). Nerve growth cone guidance mediated by G protein-coupled receptors. Nat. Neurosci. *5*, 843–848.

Yancopoulos, G.D., Davis, S., Gale, N.W., Rudge, J.S., Wiegand, S.J., and Holash, J. (2000). Vascular-specific growth factors and blood vessel formation. Nature *407*, 242–248.

Zhu, Y., Yu, T., Zhang, X.-C., Nagasawa, T., Wu, J.Y., and Rao, Y. (2002). Role of the chemokine SDF-1 as the meningeal attractant for embryonic cerebellar neurons. Nat. Neurosci. *5*, 719–720.